Robust Incision of Benoz[*a*]pyrene-7,8-dihyrodiol-9,10-epoxide−DNA Adducts by a Recombinant Thermoresistant Interspecies Combination UvrABC Endonuclease System†

Guo Hui Jiang,[#] Milan Skorvaga,[§,‡] Deborah L. Croteau,[§] Bennett Van Houten,[§] and J. Christopher States*[,#]

Department of Pharmacology and Toxicology, Brown Cancer Center, and Center for Genetics and Molecular Medicine, University of Louisville, Louisville, Kentucky 40202, Cancer Research Institute, Slovak Academy of Sciences, Vlarska 7, 833 91 Bratislava, Slovakia, and National Institute of Environmental Health Sciences, Research Triangle Park, North Carolina 27709

Received December 9, 2005; Revised Manuscript Received April 21, 2006

ABSTRACT: Prokaryotic DNA repair nucleases are useful reagents for detecting DNA lesions. UvrABC endonuclease, encoded by the *UvrA*, *UvrB*, and *UvrC* genes can incise DNA containing bulky nucleotide adducts and intrastrand cross-links. *UvrA*, *UvrB*, and *UvrC* were cloned from *Bacillus caldotenax (Bca)* and *UvrC* from *Thermatoga maritima (Tma)*, and recombinant proteins were overexpressed in and purified from *Escherichia coli*. Incision activities of UvrABC composed of all *Bca*-derived subunits (UvrABC^{Bca}) and an interspecies combination UvrABC composed of *Bca*-derived UvrA and UvrB and *Tma*-derived UvrC (UvrABC^{Tma}) were compared on benoz[*a*]pyrene-7,8-dihyrodiol-9,10-epoxide (BPDE)-adducted substrates. Both UvrABC^{Bca} and UvrABC^{Tma} specifically incised both BPDE-adducted plasmid DNAs and site-specifically modified 50-bp oligonucleotides containing a single (+)-*trans*- or (+)-*cis*-BPDE adduct. Incision activity was maximal at 55−60 °C. However, UvrABC^{Tma} was more robust than UvrABC^{Bca} with 4-fold greater incision activity on BPDE-adducted oligonucleotides and 1.5-fold greater on [^{3}H]-BPDE-adducted plasmid DNAs. Remarkably, UvrABC^{Bca} incised only at the eighth phosphodiester bond 5′ to the BPDE-modified guanosine. In contrast, UvrABC^{Tma} performed dual incision, cutting at both the fifth phosphodiester bond 3′ and eighth phosphodiester bond 5′ from BPDE-modified guanosine. BPDE adduct stereochemistry influenced incision activity, and *cis* adducts on oligonucleotide substrates were incised more efficiently than *trans* adducts by both UvrABC^{Bca} and UvrABC^{Tma}. UvrAB−DNA complex formation was similar with (+)-*trans*- and (+)-*cis*-BPDE-adducted substrates, suggesting that UvrAB binds both adducts equally and that adduct configuration modifies UvrC recognition of the UvrAB−DNA complex. The dual incision capabilities and higher incision activity of UvrABC^{Tma} make it a robust tool for DNA adduct studies.

UvrABC endonuclease is a DNA repair nuclease consisting of three subunits encoded by the *UvrA*, *UvrB*, and *UvrC* genes. This damage-specific endonuclease incises DNA containing a wide variety of structurally unrelated lesions, including bulky chemical DNA adducts and intrastrand cross-links (*1*−*4*). This system has been widely used for specifically detecting and mapping DNA adducts in human genes. Until recently, the only available UvrABC endonuclease has been from *Escherichia coli*. A major disadvantage of *E. coli* UvrABC endonuclease is its thermal instability, especially the UvrA and UvrC subunits (*5*). This limited stability leads to difficulty in estimating incision efficiency and quantitative adduct detection.

To develop a more stable reagent with greater utility for DNA adduct detection, UvrABC endonuclease subunits were cloned from the thermophilic eubacteria *Bacillus caldotenax* (*Bca*) and *Thermatoga maritima (Tma)*, organisms that have the remarkable property of growing at a temperature of 70 °C or above (*6*, *7*). Individual recombinant protein subunits were overexpressed in and purified from *E. coli*. DNA adducted by the highly reactive and mutagenic metabolite of benzo[*a*]pyrene [(+)-7*R*,8*S*-dihydroxy-9*S*,10*R*-epoxy-7,8,9,10-tetrahydrobenzo[*a*]pyrene (BPDE)] (*8*, *9*) was used as a substrate to characterize the specific incision activity of recombinant *Bca* UvrABC (UvrABC^{Bca}) and interspecies combination of *Bca* UvrAB with *Tma* UvrC (UvrABC^{Tma}). We also used BPDE adduct stereochemistry as a tool to investigate the dependence on helix distortion in repair of DNA adducts by both thermoresistant UvrABC endonucleases by digesting oligonucleotide substrates site-specifically modified with (+)-*cis*- and (+)-*trans*-BPDE adducts. Efficient detection of BPDE−DNA adducts induced in human cells is very important for environmental carcinogen and cancer prevention studies. The results show that thermoresistant UvrABC^{Bca} and UvrABC^{Tma} are stable endonu-

† This work was supported in part by USPHS Grants R01ES06460 and R01ES011314 and by the Intramural Research Program of the NIEHS, NIH.

* Corresponding author: J. Christopher States, Ph.D., Department of Pharmacology and Toxicology, University of Louisville, 570 S. Preston St., Suite 221 Louisville, KY 40202. Phone: 502-852-5347. Fax: 502-852-2492. E-mail: jcstates@louisville.edu.

[#] University of Louisville.

[§] National Institute of Environmental Health Sciences.

[‡] Slovak Academy of Sciences.

10.1021/bi052515e CCC: $33.50
Published on Web 05/28/2006

cleases with great utility for detecting BPDE−DNA adducts; both UvrABC^{Bca} and UvrABC^{Tma} preferentially incised *cis*-BPDE-adducted DNA. The interspecies combination of UvrABC^{Tma} not only makes a more robust endonuclease but confers a dual incision capability not observed with UvrABC^{Bca}.

MATERIALS AND METHODS

Cloning, Overexpression, and Purification of Bca UvrA, UvrB, and UvrC and Tma UvrC and Mutant Bca UvrC. Bca UvrA, UvrB, and UvrC proteins were overexpressed in *E. coli* cells and purified individually following the T7 IMPACT system manual (NEB) with some modifications as described previously in detail (*10*). *Tma* UvrC was cloned, overexpressed, and purified using the same procedures used for *Bca* UvrC. The QuickChange Site-Directed mutagenesis kit (Stratagene) was used to generate the plasmids encoding the *Bca* UvrC mutants. The following primer sets were used in conjunction with the parent vector, pTXB1-uvrC^{Bca} to prepare the indicated mutants: GGAGCAGCCGGGCGTGTATTTGATGAAAGAC and GTCTTTCATCAAATACACGCCCGGCTGCTCC for C18V; AAGTCGCTGAAAAATCGTGTCCGCTCGTAT and ATACGAGCGGACACGATTTTTCAGCGACTTC for E41R; CGAAGTCGCTGAAAAAACGTGTCCGCTCGTATT and AATACGAGCGGACACGTTTTTTCAGCGACTTCG for E41K. Correct clones were selected by sequencing to confirm that the mutation had been introduced. The mutant forms of pTXB1-uvrC^{Bca} were transformed into BL21(DE3) RIL cells (Stratagene). Mutants of *Bca* UvrC were overexpressed and purified using the same procedures used for wild-type (Wt) *Bca* UvrC. The proteins were maintained at −20 °C in storage buffer (50 mM Tris-HCl, pH 8.5, 500 mM KCl, 0.1 mM EDTA and 50% glycerol).

Preparation of BPDE-Damaged Plasmid DNA. [^{3}H](+)-7*R*,8*S*-dihydroxy-9*S*,10*R*-epoxy-7,8,9,10-tetrahydrobenzo[*a*]-pyrene ([^{3}H]BPDE, specific activity 1120 mCi/mmol) was obtained from the NCI Chemical Carcinogen Repository (Chemsyn, Kansas City, MO) and handled according to manufacturer's safety instructions. [^{3}H]BPDE-adducted Form I plasmid DNAs (pTHQB04, containing a 1.5-kbp fragment of the human β-globin gene; pTHQ008, containing a 1.8-kbp fragment of the human *p53* gene) were prepared as described previously (*10*). Briefly, DNAs were incubated with [^{3}H]BPDE or tetrahydrofuran (THF, [^{3}H]BPDE stock solvent) in TE buffer [10 mM Tris-HCl pH 7.5, 1 mM Na_2-EDTA] 16 h at 37 °C. Unbound [^{3}H]BPDE and its hydrolysis products were removed by ethyl acetate extraction (*11*). The extent of DNA adducts formed by [^{3}H]BPDE in plasmid DNAs was determined by scintillation spectrometry.

Plasmid Relaxation Assay. Cleavage of [^{3}H]BPDE−DNA substrates was monitored by following the conversion of plasmids from Form I to Form II in a plasmid relaxation assay as described (*10*). Briefly, [^{3}H]BPDE-treated substrates (20 fmol, equivalent to 71 ng of pTHQB04 and 75 ng of pTHQ008) were incubated with UvrA, UvrB, and UvrC in 20 μL of UvrABC buffer (50 mM Tris-HCI, pH 7.5, 50 mM KCI, 10 mM $MgCI_2$, 5 mM DTT, 1 mM ATP). Forms I and II were resolved by 1% agarose gel electrophoresis and visualized by staining with SYBR-Gold (Molecular Probes, Eugene Oregon, USA). Fluorescence emitted by SYBR-Gold of resolved bands was quantified using fluorescence detection mode (Blue excitation, 537 nm) of a Molecular Dynamics Storm 860 PhosphorImager (Amersham Pharmacia Biotech Inc. Piscataway, NJ). The average numbers of incisions and incision efficiencies were calculated using a Poisson distribution (*10*).

Preparation of Oligonucleotide Substrates. (a) DNA Substrates Containing Stereoisomeric BPDE Adducts. Adducted oligonucleotides (11-mers site-specifically modified with (+)-*trans*- and (+)-*cis*-*anti*-BPDE adducts) were the kind gifts of Dr. Nicholas Geacintov, NYU. The (+)-*trans*-, (+)-*cis*-, and no BPDE control 11-mers were ligated with equal moles of a 19-mer and a 20-mer in the presence of equal moles of the complementary 50-mer strands as described (*12*, *13*). The (+)-*anti*-BPDE-N^2-dG-adducted strand was labeled with [^{32}P] internally 21 bp from the 5′ end or 19 bp from the 3′ end, at the 3′- end or at the 5′ end as indicated in Figure 4. To construct the substrate labeled 21 bp from the 5′ end, the 11-mers [(+)-*trans*, (+)-*cis*, or no BPDE] were 5′-phosphorylated using γ-[^{32}P]ATP and T4 polynucleotide kinase, and the 19-mer was 5′-phosphorylated using unlabeled ATP and T4 polynucleotide kinase prior to assembly. To construct the substrate labeled 19 bp from the 3′ end, the 19-mer was 5′-phosphorylated using γ-[^{32}P]ATP and T4 polynucleotide kinase, and 11-mers [(+)-*trans*, (+)-*cis*, or no BPDE control] were 5′-phosphorylated using unlabeled ATP and T4 polynucleotide kinase prior to assembly. To construct 5′end-labeled substrate, the 20-mer was replaced by a 19-mer (ACTACGTACTGTTACGGCT; 20-mer with 5′ G deleted) to produce an overhanging end to prevent self-ligation of 5′-end-labeled double-stranded oligonucleotides. This 19-mer (20-mer with 5′ G deleted) was 5′-phosphorylated using γ-[^{32}P]ATP and T4 polynucleotide kinase, and 11-mers [(+)-*trans*, (+)-*cis*, or no BPDE control] and a right-hand 19-mer were 5′-phosphorylated using unlabeled ATP and T4 polynucleotide kinase. To construct a 3′ end-labeled substrate, the 19-mer was replaced by an 18-mer (GCAATCAGGCCAGATCTG; 19-mer with 3′ C deleted). The 18-mer and 11-mer [(+)-*trans*, (+)-*cis*, or no BPDE control] were 5′-phosphorylated using unlabeled ATP. Phosphorylated *trans*, (+)-*cis*, or control 11-mers were ligated with equal moles of phosphorylated 18-mer and unphosphorylated 20-mer in the presence of equal moles of the complementary 50-mer strand. The ligated oligonucleotides were modified with α-[^{32}P]dCTP at the 3′ end in the presence of Klenow DNA polymerase (*14*). [^{32}P]-labeled 49- or 50-mers (5′-end-labeled substrate is a 49-mer oligo) were purified by electrophoresis in a 12% polyacrylamide gel containing 7.5 M urea and were reannealed with fresh 50-mer complementary strand (bottom strand, Figure 4). The constructed 50-bp substrates were purified by electrophoresis in a nondenaturing 10% polyacrylamide gel containing 1× TBE.

(b) Oligonucleotide Substrates Containing Fluorescein (FldT) Adduct. DNA substrates were synthesized by Sigma-Genosys (Woodlands, TX). The DNA sequence of the 50-mer double-stranded substrate containing a single internal fluorescein (FldT) adduct was F_{26}, (GACTACGTACTGTTACGGCTCCATC[FldT]CTACCGCAATCAGGCCAGATCTGC), while the nondamaged complementary bottom strand was NDB, (GCAGATCTGGCCTGATTGCGGTAGCGATGGAGCCGTAACAGTACGTAGTC). The F_{26}, 50-mer

strand was either 5′ end-labeled or 3′ end-labeled. The 5′ end-labeling used Optikinase (USB) and γ-[^{32}P]ATP (3000 Ci/mmol, Amersham Biosciences) according to standard procedures, while the 3′ end-labeling was achieved by using Terminal transferase (Roche) and α-[^{32}P]dideoxyATP. The reactions were terminated by the addition of EDTA (20 mM), and the enzymes were heat denatured by incubation for 10 min at 65 °C. Unincorporated radioactive nucleotides were removed by gel filtration chromatography (Biospin-6, Bio-Rad). The labeled oligonucleotide was annealed with the complementary oligonucleotide using equimolar amounts. The double-stranded character of the oligonucleotide duplex was analyzed on a native 10% polyacrylamide gel.

UvrABC Incision of Oligonucleotide Substrates. (a) UvrABC Incision of Oligonucleotide Substrates Containing (+)-anti-BPDE Stereoisomeric Adducts. Substrates of 50 bp (20 fmol) were preincubated with *Bca* UvrA (10 nM) and UvrB (250 nM) at 60 °C for 30 min. *Bca* UvrC or *Tma* UvrC was added to 100 nM, and the reactions were incubated for an additional 60 min or as indicated in figures at 60 °C in 20 μL of UvrABC buffer. To investigate the temperature dependence of incision, experiments were performed under the following conditions: preincubation with 10 nM UvrA plus 250 nM UvrB at selected temperatures from 37 to 60 °C for 30 min, then UvrC was added to 100 nM, and reactions were continued at the same temperatures for 30 min as indicated in Figure 2. Time courses of specific incision by UvrABC^{Bca} and UvrABC^{Tma} on *trans*- and *cis*-BPDE-damaged 50-bp oligonucleotide substrates were examined in a kinetic assay at 37 and 60 °C (Figure 3). For the time course of incision, UvrABC reactions were performed with 20 fmol of substrates and reactions conducted at 37 and 60 °C. Substrates were preincubated with 10 nM UvrA and 250 nM UvrB for 30 min, then UvrC was added to 100 nM, and the incubation was continued for selected times from 0 to 60 min as indicated in Figure 3. Reactions were terminated by adding 2 μL of stop buffer (1% SDS, 200 mM EDTA-Na_2). DNAs were precipitated by the addition of 1/10 vol 3 M Na-acetate (pH 5.7) and 2.5 vol 95% ethanol, and precipitates were collected by centrifugation. The pellets were redissolved in 96% formamide loading buffer (96% formamide, 0.05% xylene cyanole, 0.05% bromphenol blue, 10 mM Na_2EDTA). DNAs were denatured at 90 °C for 5 min and resolved by electrophoresis in denaturing 15% polyacrylamide gel containing 7.5 M urea in 1× TBE buffer (89 mM Tris, 89 mM boric acid, 10 mM EDTA, pH 8.4). Resolved band intensities were quantitated with a Molecular Dynamics Storm 860 PhosphorImager and Imagequant software.

(b) UvrABC Incision of DNA Substrates Containing Fluorescein (FldT) Adduct. Prior to initiation of the incision assay, the UvrABC proteins were heated to 65 °C for 10 min. The 5′ or 3′ end-labeled duplex DNA (2 nM, F_{26}50/NDB) was treated with Wt UvrABC or UvrAB with mutant *Bca* UvrC (20 nM *Bca* UvrA, 100 nM *Bca* UvrB and 50 nM *Bca* UvrC) in 20 μL of UvrABC buffer (50 mM Tris-HCl pH 7.5, 50 mM KCl, 10 mM $MgCl_2$, 1 mM ATP, and 5 mM DTT) at 55 °C for the 30 min. The reactions were terminated by the addition of EDTA (20 mM). The DNA from the reaction was denatured by the addition of formamide and heating to 85 °C for 5 min. Incision products were resolved on a 10% denaturing polyacrylamide gel, and electrophoresis was performed at 325 V in 1× TBE buffer for 40 min. Gels were dried and exposed to a phosphorImager screen (Molecular Dynamics) overnight. The percent of the DNA incised was calculated using the band intensities within the lane and the Molecular Dynamics software, ImageQuant.

Binding Affinity Assay of UvrA or UvrAB to (+)-anti-BPDE Stereoisomeric Adducts. To investigate the role of BPDE adduct stereochemistry on the repair of DNA adducts, the binding affinity of UvrA or UvrA /UvrB with (+)-*trans*- and (+)-*cis*-BPDE-adducted substrates was examined. [^{32}P]-labeled DNA substrates (1 nM) containing stereospecific adducts were incubated with *Bca* UvrA alone or UvrA plus UvrB at 60 °C for 30 min in a 10 μL reaction containing UvrABC buffer. Following incubation, 2 μL of 80% glycerol was added, and the mixture was immediately loaded onto a 4% native polyacrylamide gel containing 1× TBE buffer plus 1 mM ATP and 10 mM $MgCl_2$ and run at 4 °C. The binding ratios of UvrA or UvrAB with (+)-*trans*- or (+)*cis*-BPDE substrates were quantitated with a Molecular Dynamics Storm 860 PhosphorImager and Imagequant software.

RESULTS

UvrA, UvrB, and UvrC Expression and Purification. Purification of recombinant *Bca* UvrA, UvrB, and UvrC subunits was reported elsewhere (*10*). *Tma* UvrC was cloned, overexpressed in *E. coli*, and purified using a similar approach. The activities of UvrC from *Bca* and *Tma* were compared when used in conjunction with *Bca* UvrA and UvrB. The resulting endonuclease systems are referred to as UvrABC^{Bca} and UvrABC^{Tma}.

Incision Capability of UvrABC^{Bca} and UvrABC^{Tma} on BPDE-Damaged Plasmid DNAs. A plasmid relaxation assay was used to compare incision capacities of UvrABC^{Bca} and UvrABC^{Tma} endonucleases. When adducts formed on supercoiled DNA are incised by UvrABC nucleases, the DNA helix is relaxed and Form I DNA (supercoiled) is changed to Form II (nicked/open circular DNA). The two forms are readily resolved by agarose gel electrophoresis. Two plasmids (pTHQB04 and pTHQ008) were used as substrates for UvrABC incision assays. Plasmid DNAs untreated (THF control) and treated with [^{3}H]BPDE to form two adducts per plasmid molecule (*10*) were used as substrates for the cleavage reactions. The substrates were incubated with UvrABC^{Bca} or UvrABC^{Tma} with UvrC at 0, 12.5, or 25 nM as indicated in Figure 1. Maximal activity for each was achieved with UvrC at 25 nM. Specific incision on [^{3}H]-BPDE-damaged pTHQ008 was 48% with UvrABC^{Bca}. Substitution of UvrABC^{Tma} for UvrABC^{Bca} increased incision to 70%. Incision of UvrABC^{Bca} on [^{3}H]BPDE-damaged pTHQB04 was 41%, while reactions with UvrABC^{Tma} exhibited incision of 58%. Thus, UvrABC^{Tma} appears to be more active than UvrABC^{Bca} on BPDE-adducted plasmid DNAs.

Temperature-Dependent Incision of UvrABC^{Bca} and UvrABC^{Tma} on BPDE-Adducted DNAs. To demonstrate the thermophilic character UvrABC^{Bca} and UvrABC^{Tma} incision activity, the temperature dependence of incision was determined. Oligonucleotides (50-mers) containing either a (+)-*cis*-, a (+)-*trans*-, or no BPDE adduct in one strand were site-specifically labeled (internally 19 bp from the 3′ end of 50-bp substrates) with [^{32}P] and used as substrates for UvrABC endonuclease. Incision by UvrABC^{Bca} produced a

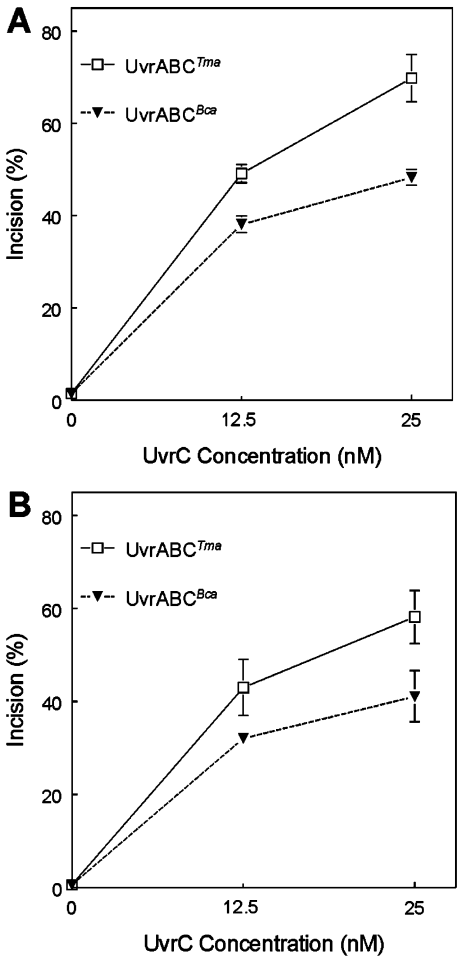

FIGURE 1: Incision of [^{3}H]BPDE-treated plasmids by UvrABC^{Tma} and UvrABC^{Bca}. (A) [^{3}H]BPDE-treated pTHQ008. (B) [^{3}H]BPDE-treated pTHQB04. Plasmids pTHQ008 and pTHQB04 treated with (+)-*anti*-[^{3}H]BPDE (2 lesions/plasmid) were used as substrates for UvrA, UvrB, and UvrC in a plasmid relaxation assay. Twenty femtomoles of DNA substrate were incubated with UvrABC in 20 μL of UvrABC buffer. *Bca* UvrA (2.5 nM) and *Bca* UvrB (62.5 nM) were held constant. *Tma* UvrC and *Bca* UvrC concentrations were varied as indicated. Form I and Form II plasmids were resolved by agaraose gel electrophoresis and quantitated, and the average incision was calculated by applying the Poisson distribution and expressed as % of lesions incised. Means ± SD from quadruplicates reactions are plotted.

32-nucleotide fragment (5′ incision only), whereas incision by UvrABC^{Tma} produced a 20-nucleotide fragment (3′ incision monitored). Efficient incision required increased UvrABC concentration up to 4-fold as compared to reaction conditions with BPDE-damaged plasmid DNAs. Incision activity was temperature-dependent and reached a plateau at 55−60 °C (Figure 2). At 37 °C, both UvrABC^{Bca} and UvrABC^{Tma} exhibited low incision activity. At all temperatures monitored, both UvrABC^{Bca} and UvrABC^{Tma} incised *cis*-BPDE-adducted DNA substrates more than *trans*-BPDE-adducted DNA substrates. Incision by UvrABC^{Tma} was 3−4-fold greater than incision by UvrABC^{Bca} at all temperatures and on both substrates.

Time Course of Specific Incision of UvrABC^{Bca} and UvrABC^{Tma} on trans- and cis-BPDE-Damaged DNA. The selectivity of UvrABC^{Bca} and UvrABC^{Tma} for damaged DNAs was examined further by testing the ability of UvrABC specifically to recognize and to incise (+)-*trans*-

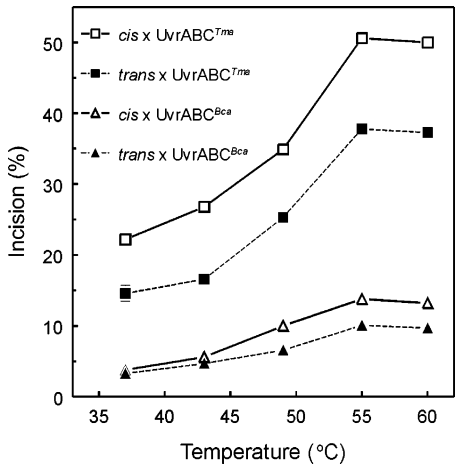

FIGURE 2: Temperature-dependent incision of *trans*- and *cis*-BPDE-adducted oligonucleotide substrates UvrABC^{Tma} and UvrABC^{Bca}. *trans*- and *cis*-BPDE-adducted 50-bp double-stranded oligonucleotides labeled internally 19 bp from the 3′ end (1 nM) were preincubated with UvrA (10 nM) and UvrB (250 nM) for 30 min at 37, 43, 49, 55, or 60 °C as indicated. UvrC^{Tma} or UvrC^{Bca} was added to 100 nM, and the reaction was incubated for an additional 30 min at the indicated temperatures. Reaction products were denatured and resolved by electrophoresis in 12% polyacrylamide gels containing 7.5 M urea. The intensities of the resolved bands were quantitated, and the average incision ratio was calculated. Means ± SD from triplicate reaction are plotted.

and (+)-*cis*-BPDE-damaged 50-bp oligonucleotide substrates in a kinetic assay (Figure 3). The time course of lesion-specific incision was determined at 37 and 60 °C. Oligonucleotides containing either a *cis*-, a *trans*- or no BPDE adduct were site-specifically labeled with [^{32}P] 19 bp from the 3′ end to monitor incision (5′ incision for UvrABC^{Bca}, producing a 32-mer fragment; 3′ incision for UvrABC^{Tma}, producing a 20-mer fragment). Incision activities of both UvrABC^{Bca} and UvrABC^{Tma} were time dependent on both (+)-*trans*- and (+)-*cis*-BPDE DNA substrates. Incision continued to increase for at least 60 min at 60 °C. Incision was less robust at 37 °C for both UvrABC^{Bca} and UvrABC^{Tma}. Incision was not observed on control substrates that did not contain a BPDE adduct. Incision activity of UvrABC^{Tma} was about 3.5-fold greater than UvrABC^{Bca}. Again, both UvrABC^{Bca} and UvrABC^{Tma} showed greater incision activity on (+)-c*is*-BPDE-adducted substrates than on (+)-*trans*-BPDE-adducted substrates.

UvrABC^{Tma} Exhibits Dual Incision Capability Not Present In UvrABC$^{Bca.}$ As noted above, UvrABC^{Bca} incised only 5′ of the lesion, whereas UvrABC^{Tma} incised 3′ of the lesion. To map the specific incision sites and to demonstrate that UvrABC^{Tma} performed dual incision, (+)-*trans*, (+)-*cis*, and no BPDE 50-bp substrates were constructed and labeled on the (+)-*anti*-BPDE-N^2-dG-adducted strand with [^{32}P] either internally 21 bp from the 5′ end, internally 19 bp from the 3′ end, at the 3′- end or at the 5′ end (49/50-mer, see Methods, *Preparation of BPDE-Damaged Plasmid DNA*). The results of incision of substrates labeled internally 21 bp from the 5′ end, internally 19 bp from the 3′ end, and at the 3′ end showed that UvrABC^{Bca} only produces a 32-mer fragment from substrates labeled at all three sites (Figure 4A−C). The results of incision of substrates labeled at the 5′ end showed that UvrABC^{Bca} only produces a 17-mer fragment (Figure 4D). These results indicate that *Bca* UvrC only incises at the eighth phosphodiester bond 5′ to the

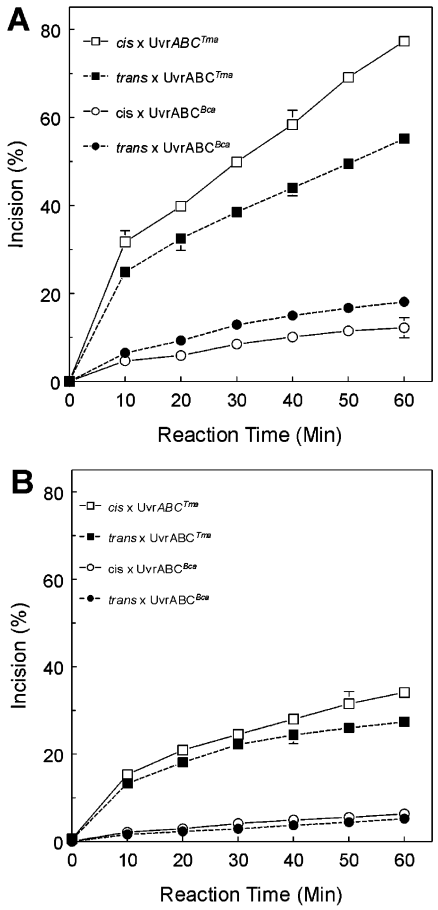

FIGURE 3: Time course of UvrABC^{Tma} and UvrABC^{Bca} incisions of *trans*- and *cis*-BPDE-adducted oligonucelotide substrates. (A) 60 °C. (B) 37 °C. Oligonucleotides containing either a *cis*-, a *trans*-, or no BPDE adduct were site-specifically labeled with [^{32}P] internally 19 bp from the 3′ end to monitor the 5′ incision (producing a 32-mer fragment) for UvrABC^{Bca} and 3′ incision (producing a 20-mer fragment) for UvrABC^{Tma}, labeled 50-bp oligonucleotides were used as substrates in UvrABC reactions. UvrABC reactions were performed with twenty femtomoles of substrates. Preincubation of substrates with UvrA 10 nM and UvrB 250 nM for 30 min at 60 °C, then added UvrC (100 nM) with incubation at varied time as indicated in the figure. Reaction products were denatured and resolved on 12% polyacrylamide sequencing gel. The intensities of the resolved bands were quantitated, and the average incision ratio was calculated. Means ± SD from triplicate reactions are plotted.

BPDE-modified guanosine. In contrast, UvrABC^{Tma} generates different patterns with different sites of labeling (Figure 4A−D). UvrABC^{Tma} incision of oligonucleotides labeled 19 bp from the 3′ end or at the 3′ end generates a doublet corresponding to 19- and 20-mers (Figure 4A,C). A 12-mer is released by incision of oligonucleotides labeled 21 bp from the 5′ end (Figure 4B). A 17-mer fragment is produced by *Tma* UvrC incision of substrates labeled at the 5′ end (Figure 4D). These results indicate that UvrABC^{Tma} performs dual incision, cutting both the fifth phosphodiester bond 3′ and the eighth phosphodiester bond 5′ from BPDE-modified guanosine.

Interrelation of UvrABC^{Tma} and UvrABC^{Bca} in UvrABC Incision Reaction. To investigate the potential interaction between *Tma* UvrC and *Bca* UvrC in the UvrABC incision reaction, *Tma* UvrC and *Bca* UvrC were added individually, sequentially, or concurrently to the reactions after preincubation of substrate oligos with *Bca* UvrA and UvrB (Figure 5). Incision on *cis*-BPDE-adducted oligonucelotides was monitored with substrates [^{32}P]-labeled 19 bp from the 3′ end. Incision 5′ to the adducted nucleotide without 3′ incision yields a labeled 32-mer. Incision 3′ of the adducted nucleotide (with or without 5′ incision) yields a labeled 20-mer. *Bca* UvrC alone yielded the 32-mer as seen previously. Likewise, *Tma* UvrC alone yielded only the 20-mer product and in greater yield than the *Bca* UvrC-generated 32-mer product. Sequential incubation with *Tma* UvrC followed by *Bca* UvrC yielded a 20-mer in amounts equal to *Tma* UvrC alone and a small amount of 32-mer. This result suggests that *Bca* UvrC incised a small number of substrates not incised by *Tma* UvrC. Sequential incubation first with *Bca* UvrC then with *Tma* UvrC also yielded both 32-mer and 20-mer bands. However, both were less intense than that observed with either *Bca* UvrC or *Tma* UvrC alone. Reduction in 32-mer generated by *Bca* UvrC after the addition of *Tma* UvrC suggests that *Tma* UvrC is making a 3′ incision on substrates already incised 5′ of the lesion by *Bca* UvrC. Concurrent addition of *Bca* UvrC and *Tma* UvrC yielded both the 32-mer and the 20-mer. However, although the 20-mer was more intense than the 32-mer, the intensities of both bands were less than with either UvrC alone. This result suggests that the *Tma* UvrC clearly is more active than the *Bca* UvrC; the two UvrC's do not cooperate and may interfere with each other.

UvrA and UvrAB Recognize and Bind Both (+)-trans- and (+)-cis-BPDE-Modified Substrates with Equal Affinity. Incision of *cis*-BPDE-adducted substrates was greater than incision of *trans*-BPDE-adducted substrates by both UvrABC^{Bca} and UvrABC^{Tma}. To investigate whether the BPDE stereochemistry affected repair by altering recognition of the lesion by UvrA or in loading UvrB by UvrAB, the binding affinity of UvrA and UvrA plus UvrB with *trans*- and *cis*-BPDE-adducted substrates was examined by the electrophoretic mobility shift assay (EMSA).

UvrA−DNA complex formation was the same for both (+)-*cis*- and (+)-*trans*-BPDE-adducted substrates (Figure 6A). Likewise, UvrAB complex formation also was the same for the two substrates (Figure 6B). These results indicate that the UvrAB complex recognizes and binds both adducts with equal affinity and that UvrA and UvrAB do not distinguish between *cis*- and *trans*-BPDE adducts. Thus, the preferential incision of (+)-*cis*-BPDE adducts suggests that adduct configuration modifies the recognition of the UvrB−DNA lesion complex by both *Bca* and *Tma* UvrC.

The Bca UvrC Mutants Exhibit 5′ Incision Properties Similar to Wt Bca UvrC. (a) Analysis of the Bca UvrC Amino Acid Sequence. Comparison of the *Bca* UvrC sequence to 22 UvrC proteins, including *Tma* and *E. coli* UvrC, revealed several differences in the N-terminal nuclease domain, specifically at Cys18 and Glu39 of the *Bca* UvrC sequence. An alignment of *Bca* UvrC, *Tma* UvrC, and *E. coli* UvrC is depicted in Figure 7. Within the *Bca* UvrC sequence, Cys18 lies within the first conserved element of the GIY−YIG endonuclease domain; however, among UvrCs, Val is the most common amino acid between the absolutely conserved Gly and Tyr. Unlike almost all other UvrC sequences, *Bca* UvrC contains an acidic amino acid, Glu39, adjacent to the catalytic Arg, Arg40. We hypothesized that these amino acids may interfere with the 3′ incision event, and therefore via

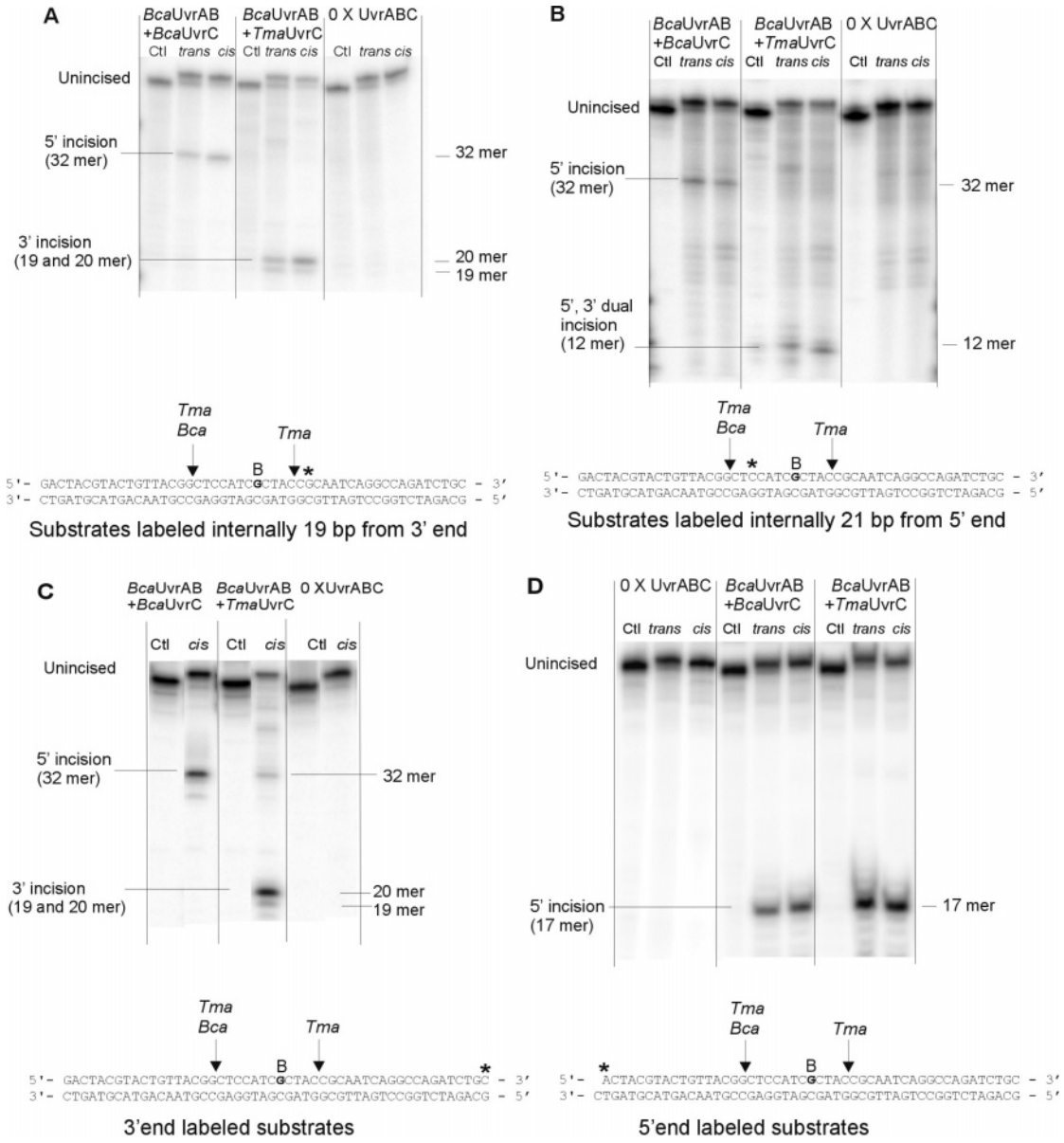

FIGURE 4: Incision maps of UvrABC^{Bca} and UvrABC^{Tma} on BPDE-adducted oligonucleotide substrates. (A) Substrates labeled internally 19 bp from the 3′ end. (B) Substrate labeled internally 21 bp from the 5′ end. (C) Substrate labeled at the 3′ end. (D) Substrate labeled at the 5′ end. BPDE-modified 50-bp double-stranded oligonucleotides (1 nM) labeled at different sites were preincubated with UvrA (10 nM) and UvrB (250 nM) for 30 min at 60 °C, *Tma* UvrC or *Bca* UvrC (100 nM) was added, and the incubation was continued at 60 °C for 60 min. Reaction products were denatured and resolved by electrophoresis in 15% polyacrylamide gels containing 7.5 M urea.

site-directed mutatagenesis these amino acids were converted to the most common amino acids present at these position. The amino acid changes were Cys18Val, Glu39Asn, and Glu39Lys. The recombinant proteins were purified as described for the Wt proteins, and an image of the proteins is shown in Figure 8A.

(b) Oligonucleotides Incision Assays of Wt and Mutated Bca UvrC. Oligonucleotide incision assays were performed with Wt *Tma*, Wt *Bca*, and mutant *Bca* UvrC proteins to compare the incision patterns and relative activity (Figure 8). The DNA substrate was a FldT-adducted thymine centrally located within a 50-bp duplex. As shown in Figure 8B,C, the *Tma* and the *Bca* UvrC proteins created the same incision pattern when the DNA was 5′ end-labeled with [^{32}P], a 18-nucleotide product. Curiously, Wt *Bca* UvrC possessed about 25% of the incision activity as Wt *Tma*, while the mutants ranged between 31 and 51%. When the DNA was labeled at the 3′ end of the duplex with [^{32}P], the *Bca* UvrC proteins failed to make the expected 3′ cut, because a 20-bp product was expected, while a 32-bp product is observed. This is consistent with the observation that *Bca* UvrC makes the incision only on the 5′ side of the DNA lesion, while *Tma* UvrC makes the dual incision (Figure 8D). Therefore, the *Bca* UvrC amino acids Cys18 and Glu39 play no role in determining whether the 3′ cut will occur.

DISCUSSION

Nucleotide excision repair (NER) is the major pathway that removes UV photoproducts and "bulky" chemical adducts from DNA. In prokaryotes, lesion recognition and excision are performed by the UvrABC endonuclease. UvrABC endonuclease detects and removes DNA damage induced by a wide range of chemical carcinogens. UvrABC consists of three subunits (UvrA, UvrB, UvrC) that act

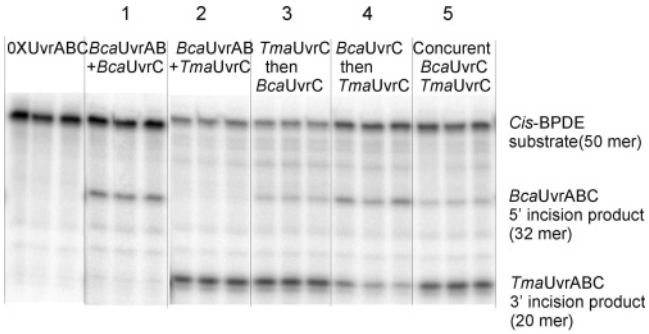

FIGURE 5: The interrelation of UvrABC^{Tma} and UvrABC^{Bca} in UvrABC incision reaction. UvrABC incision reactions were performed in UvrABC buffer with subunit UvrA (10 nM), UvrB (250 nM), and UvrC (100 nM) in the presence of ^{32}P-labeled *cis*-BPDE DNA substrates. Substrates were preincubated with *Bca* UvrAB at 60 °C for 30 min, and then *Bca* UvrC or *Tma* UvrC were individually added in reaction 1 and 2, or *Tma* UvrC and *Bca* UvrC were concurrently added in reaction 5, with incubation 60 min at 60 °C. After preincubation of UvrAB with substrates, in reaction 3, *Tma* UvrC was added and incubated for 60 min, and then *Bca* UvrC was added sequentially for an additional 60 min incubation. At reaction 4, *Bca* UvrC was added and incubated for 60 min, and then *Tma* UvrC was added sequentially for an additional 60 min incubation at 60 °C. Reaction products were denatured and resolved by electrophoresis in 15% polyacrylamide gels containing 7.5 M urea.

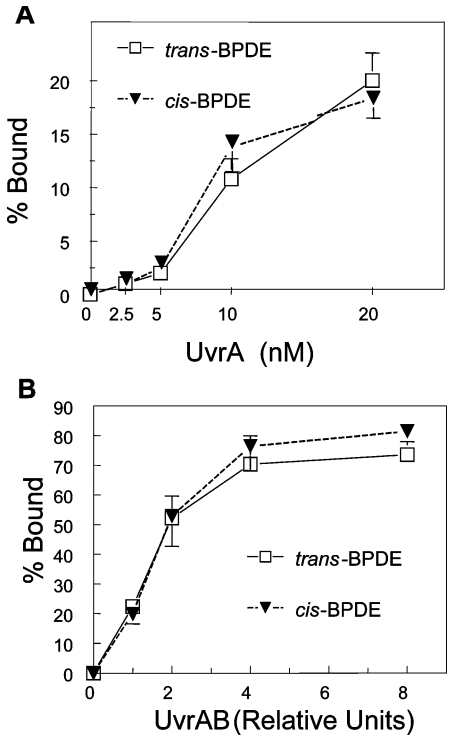

FIGURE 6: Protein−DNA complex formation with (+)-*trans*- and (+)-*cis*-BPDE-adducted oligonucleotides. (A) UvrA−DNA complex formation. (B) UvrAB−DNA complex formation. *trans*- and *cis*-BPDE-modified 50-bp double-stranded oligonucleotides (1 nM) were incubated with different concentrations of *Bca* UvrA or UvrA + UvrB as indicated in the figure. UvrA and UvrB relative units: 1 = UvrA 2.5 nM, UvrB 62.5 nM. The reaction was performed at 60 °C for 30 min in a 10 μL reaction containing 50 mM Tris-CI, pH7.5, 50 mM KCI, 10 mM $MgCI_2$, 5 mM DTT, and 1 mM ATP. The reaction samples were resolved on a 4% native polyacylamide gel run with TBE buffer containing 1 mM ATP and 10 mM $MgCI_2$ at 4 °C. The intensities of the resolved bands were quantitated, and the average binding ratios of UvrA or UvrA B with *trans*- or *cis*-BPDE substrates were calculated. Means ± SD of four independent experiments are plotted.

sequentially. Studies with *E. coli* UvrABC indicate that damage recognition begins with the dimerization of UvrA. The $UvrA_2$ dimer loads UvrB onto the lesion, resulting in a stable UvrB−DNA preincision complex at the lesion, and $UvrA_2$ is released. This model is corroborated by recent studies by Della Vecchia et al. (*15*) using *Bca* UvrA and UvrB. The UvrB−DNA preincision complex is recognized by UvrC and leads to incision of the damaged strand at the fourth or fifth phosphodiester bond 3′ to the lesion. Generally, this 3′ incision is immediately followed by hydrolysis of the eighth phosphodiester bond 5′ to the lesion to complete excision (*16*−*20*). Two notable exceptions to this paradigm have been reported. CHO, which incises only 3′ of a lesion, and UvrCII, a high salt induced *E. coli* UvrC tetramer that incises only 5′ of certain lesions. Our studies of *Bca* UvrC, which incises only 5′ of both (+)-*trans*- and (+)-*cis*-BPDE−DNA adducts, indicate a third exception to the paradigm.

Moolenaar et al (*21*, *22*) reported an *E. coli* UvrC homologue named Cho that incises only at the nineth phosphodiester bond 3′ to the modified nucleotide, four nucleotides beyond the site of the normal UvrC incision. Cho can incise some DNA lesions more efficiently than *Eco* UvrC. *Eco* UvrC can make the 5′ incision on a substrate already incised 3′ by Cho, indicating the potential for interaction between UvrC and Cho. In the present study, we observed that *Tma* UvrC could incise 3′ of the lesion on substrates already incised 5′ by *Bca* UvrC. Thus, *Tma* UvrC can complement *Bca* UvrC to make a 3′ incision that is not observed in the absence of *Tma* UvrC. Also, with sequential incubation of substrates with UvrABC^{Tma} followed by the addition of *Bca* UvrC, we found 5′ incision fragment produced by UvrABC^{Bca}, indicating incision on substrates not incised by UvrABC^{Tma}. These results raise the possibility that *Bca* UvrC might be a *Bca* homologue of UvrC with only 5′ incision activity and that another as yet unidentified UvrC homologue providing 3′ incision activity in *Bca* has not yet been identified. Thus, analogous to UvrC/Cho interaction in *E. coli*, UvrC homologues may work together for efficient dual incision on particular lesions.

Tang et al (*23*) separated two forms of *E. coli* UvrC eluting at different ionic strengths from DNA−cellulose: UvrCI (eluted with 0.4 M KCI) and UvrCII (eluted with 0.6 M KCI). The molecular weight of UvrCII is four times that of UvrCI suggesting that UvrCII is a tetramer. The specific incision activity of UvrCII is only one-fourth that of UvrCI correlating with much lower binding affinity of UvrCII than UvrCI to UvrAB−DNA complex. The sites of incision at 5′ and 3′ of a UV-induced pyrimidine dimer are same for both UvrCI and UvrCII (*23*). However, UvrCI and UvrCII have different nuclease incision activities on a CC-1605-N3-adenine adduct. UvrCI exhibits dual incision activity, cutting 5′ and 3′ of the adduct, whereas UvrCII makes only the 5′ incision (*24*). Our UvrC preparations are eluted from the chitin binding column in 2 M NaCl and dialyzed to 500 mM NaCl (*10*). It is possible that the high salt conditions are converting *Bca* UvrC but not *Tma* UvrC into a tetramer, and the tetrameric form exhibits 5′-only incision on certain DNA lesions. Tetrameric UvrCII was able to make incisions at lesions in the absence of UvrB. We have not been able to

FIGURE 7: Alignment of UvrC sequences of *E. coli*, *Bca*, and *Tma*. (A) 3′ Nuclease domain. (B) Uvr interaction domain. Amino acids shared by all three UvrC proteins are highlighted in light blue; by *E. coli* UvrC (EcoC) and *Bca* UvrC (BcaC), in yellow; by EcoC and *Tma* UvrC (TmaC), in magenta; by BcaC and TmaC, in green. Alignment performed using Clustal W. In panel A, the amino acids (C18 and E39) that were mutated in *Bca* UvrC are highlighted in red and marked with a † above the sequence. The arginine residue at position 42 in *Eco* UvrC is marked with a # in panel A.

detect tetramerization of *Bca* UvrC. Furthermore, specific incision at lesions is observed only in the presence of UvrA/UvrB (*10*).

Results of the present study show that UvrABC^{Bca} and UvrABC^{Tma} both exhibit better incision of (+)-*cis*-BPDE adducts than (+)-*trans*-BPDE adducts, similar to the preference exhibited by *E. coli* UvrABC (*13*, *14*). This differential in incision is not as great as in human nucleotide excision repair extracts (*25*). Our results combined with these earlier reports by others clearly indicate that UvrA binding affinity is not the only determinant in UvrABC recognition and excision of lesions.

(+)-*anti*-BPDE forms two stereoisomeric adducts: (+)-*trans*- and (+)-*cis*-BPDE adducts. The predominant conformation of the (+)-trans adduct has the pyrene ring system lying in the DNA minor groove (causing a minor helix distortion). The predominant conformation of the (+)-cis adduct has the pyrene ring system "intercalated" in DNA causing a major helix distortion (*26*−*29*). A widely held hypothesis is that the configurational and conformational differences play a major role in recognition of BPDE-induced DNA lesions by NER. This conformational difference is proposed to contribute to the preferential recognition of the (+)-*cis*-BPDE adduct by the NER systems of both humans and prokaryotes. To answer the question of whether poor incision of (+)-*trans*-BPDE adducts by UvrABC is caused by poor formation of UvrB−DNA preincision complex to *trans*-BPDE adducts, we tested the binding affinity of UvrA and UvrA/UvrB with *trans*- and *cis*-BPDE-adducted substrates. Neither UvrA nor UvrA/UvrB displayed differential binding affinity for (+)-*trans*- or (+)-*cis*-BPDE-modified substrates (Figure 6). This result indicates that UvrA/UvrB recognizes and binds both adducts with equal affinity. Zou et al (*14*) reported that *E. coli* UvrA and UvrB form complexes better with (+)-*cis*-BPDE-adducted DNA than with (+)-*trans*-BPDE-adducted DNA. Thus, the efficiency of incision by *E. coli* UvrABC correlated with UvrAB binding affinity for the (+) isomers. However, this correlation did not hold when comparing binding and incision of (+) and (−) isomers, suggesting that factors other than UvrAB affinity were important. In our studies, preferential incision of (+)-*cis*-BPDE adducts in the face of equal binding by *Bca* UvrAB of *trans*- and *cis*-BPDE adducts supports the suggestion that UvrC plays a final role in DNA lesion recognition. Since UvrC incision of the UvrB−DNA complex is adduct configuration dependent for both *Bca* and *Tma* UvrC, the structure of the DNA adduct appears to affect the interactions between UvrC and the UvrB/DNA complex. UvrB has ATPase and DNA helicase activity. When it binds DNA adducts, UvrB uses its helicase fold to bend the DNA and push the damaged DNA strand into the nuclease cleft in UvrC (*19*, *30*−*32*). UvrC is capable of recognizing some secondary structure, such as UvrB opened DNA complex (*18*, *31*, *33*, *34*). It is very possible that UvrC will not cut unless UvrB has bound and altered the conformation of damaged DNA, or if the DNA is not bent sufficiently to enter into the UvrC nuclease site. We propose that the (+)-*cis*-BPDE adduct may more easily adopt the preferential structure upon binding by *Bca* UvrB at the elevated temperatures of the assay, thus facilitating UvrC binding and incision. Clearly, the mechanism of UvrC discrimination between similar lesions is not well understood, and further study is needed.

The exciting discovery in this study is that interspecies use of UvrABC^{Tma} not only makes a more robust endonuclease but also confers dual incision capability (cutting at both the fourth or fifth phosphodiester bond 3′ and the eighth phosphodiester bond 5′ to BPDE-modified guanosine) not present in UvrABC^{Bca}. *Bca* UvrC incises only at the eighth phosphodiester bond 5′ to the BPDE-modified guanosine. The results were confirmed on substrates modified with both (+)-*trans*- and (+)-*cis*-BPDE [^{32}P]-labeled in four different positions. This result raises an intriguing question: why does *Bca* UvrC incise only at the eighth phosphodiester bond 5′ to the BPDE lesion but not on the 3′ side? The mechanism of UvrC incision defined with *E. coli* UvrABC is a sequential process. When UvrC recognizes UvrB−DNA preincision complex, it first incises the damaged strand at the fourth or fifth phosphodiester bond 3′ to the lesion and then immediately follows this 3′ incision by hydrolysis of the eighth phosphodiester bond 5′ to the lesion. Our results clearly show that 5′ incision is not always dependent on prior 3′ incision.

UvrC has two functional nuclease domains (*34*, *35*, *35*−*37*). The N-terminal domain is responsible for cutting the damaged strand most commonly at the fifth phosphodiester bond 3′ to the modified nucleotide, while the C-terminal domain is responsible for the second incision at the eighth phosphodiester bond 5′ to the damaged nucleotide. The N-terminal nuclease domain contains a region that interacts with a homologous domain of the UvrB (C-terminal) in the UvrBC−DNA incision complex (*35*, *36*). In *E. coli*, the C-terminal nuclease domain contains all the elements for 5′

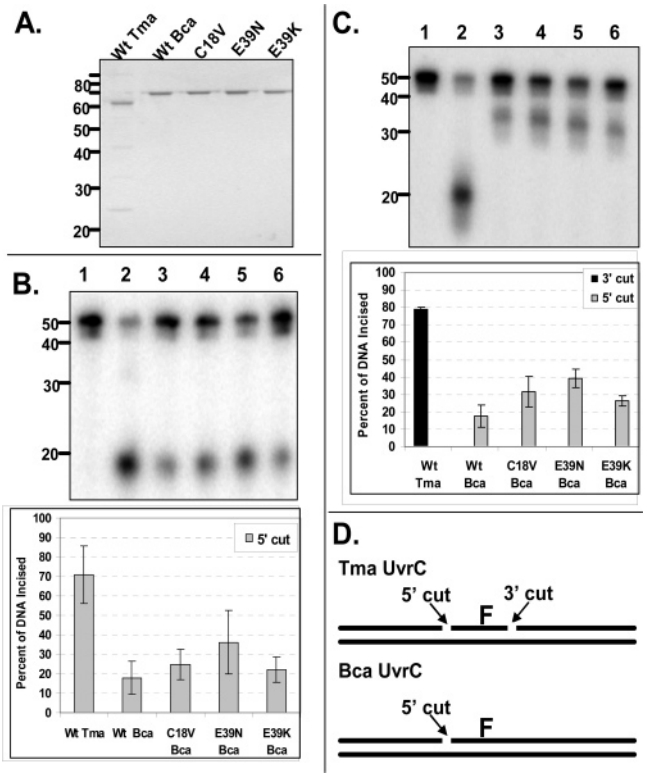

FIGURE 8: Mutation of C18 or E39 does not restore 3′ endonuclease activity. (A) Protein gel of proteins used in study. Fifteen microliters of each protein (500 nM) was applied to a 10% Tris-Bis NuPAGE gel. Electrophoresis was carried out for 55 min at 200 V. The protein gel was stained with SimplyBlue and destained with water. (B) Oligonucleotide incision products and graphic representation of the data obtained from the 5′-[^{32}P]-end-labeled duplex. The FldT-adducted 50-bp duplex (2 nM F_{26}50/NDB) was incubated with UvrA (20 nM), UvrB (100 nM), and the indicated UvrC (50 nM) at 55 °C for 30 min in reaction buffer. The reactions were terminated with stop buffer, and the incision products were analyzed on a 10% denaturing polyacrylamide gel. Graphic representation of the data is reported as the mean ± the standard deviation (n = 3). (C) Oligonucleotide incision products and graphic representation of the data obtained from the 3′-[^{32}P]-end-labeled duplex. The FldT-adducted 50-bp duplex (2 nM F_{26}50/NDB) was incubated with UvrA (20 nM), UvrB (100 nM), and the indicated UvrC (50 nM) at 55 °C for 30 min in reaction buffer. The reactions were terminated with stop buffer, and the incision products were analyzed on a 10% denaturing polyacrylamide gel. Graphic representation of the data is reported as the mean ± the standard deviation (n = 3). (D) Graphic summarizing the observed endonuclease sites produced by the different UvrC proteins. *Tma* UvrC creates the dual incision while *Bca* UvrC only makes the cut on the 5′ side of the DNA lesion.

incision (*34*, *35*). *Tma* UvrC incises with high efficiency and produces the 5′ and 3′ dual incision.

Sequence divergence between *Bca* UvrC and *Tma* UvrC may highlight residues important for 3′ nuclease activity. The region of UvrC most likely to impact 3′ incision activity is the 3′ nuclease domain. Comparison of this region in *Tma*, *Bca* and *Eco* UvrC (Figure 7A) revealed that *Bca* UvrC is more similar to *Eco* UvrC than to *Tma* UvrC. *Bca* UvrC shares all but four amino acids with *Eco* UvrC, whereas *Tma* UvrC has eight amino acid differences, three of which are at divergent positions in *Bca* UvrC. Because *Tma* UvrC and not *Bca* UvrC retains dual incision activity, one might infer that the eight divergent amino acids in the *Tma* sequence must not be essential for 3′ nuclease activity. The arginine residue at position 42 in *Eco* UvrC (marked with # in Figure 7A) is critical to 3′ nuclease activity and is flanked by divergent amino acids in *Bca* UvrC. However, the amino acid preceding is a significant change in charge (K → E) in *Bca* UvrC but changed to neutral charge (K → N) in *Tma* UvrC, whereas the following amino acid is a conservative change in *Bca* UvrC (L → V) and unchanged in *Tma* UvrC. We tested whether two of the divergent amino acids in *Bca* UvrC were responsible for the loss of 3′ incision activity. Changing neither Cys18 to Val, nor Glu39 to Asn or Lys, was able to confer 3′ incision activity on *Bca* UvrC. There are numerous other amino acid differences between *Bca* UvrC and other UvrC proteins that have dual incision activity. Extensive site-directed mutation studies are required to elucidate which of these amino acid changes are responsible for the loss of the 3′ nuclease activity in *Bca* UvrC.

It is possible that the interactions of *Bca* UvrC and *Tma* UvrC with UvrB via the Uvr domain are different, causing the respective UvrC's to align differently and thus abrogating 3′ nuclease activity in *Bca* UvrC. As shown in Figure 7B, the Uvr regions of *Bca*, *Tma*, and *Eco* UvrC share some sequence identity but diverge considerably. Again, although *Bca* is slightly less divergent from *Eco* UvrC overall than is *Tma* UvrC, there are amino acids conserved in *Tma* UvrC that are not conserved in *Bca* UvrC. The fact that we have examined functionality with *Bca* UvrA, UvrB, and UvrC and under these conditions *Bca* UvrC has only 5′ endonuclease activity suggests that *Bca* may have a second UvrC homologue analogous to *E. coli* CHO that performs the 3′ incision.

In conclusion, recombinant, thermoresistant UvrABC endonucleases composed of subunits cloned from *Bca* and *Tma* were used as analytical tools to detect BPDE−DNA adducts. The results show that both UvrABC^{Bca} and interspecies UvrABC^{Tma} specifically incise (+)-*trans*- and (+)-*cis*-BPDE−DNA adducts with greater activity on (+)-*cis*-BPDE adducts. Interestingly, the interspecies UvrABC^{Tma} not only performs dual incision but also is more active than UvrABC^{Bca}. UvrA/UvrAB complex recognizes and binds both *trans*- and *cis*-adducts with equal affinity, but UvrC from both species preferentially incises (+)-*cis*-BPDE adducts, suggesting that UvrC recognition of the UvrB−DNA lesion complex plays a final role in DNA lesion recognition. Comparison of these two UvrC proteins offers the opportunity to learn more about the specific functions of UvrC in the recognition and removal of DNA lesions.

ACKNOWLEDGMENT

The authors thank Dr. Mark Melton for technical assistance in purifying the *Bca* UvrC mutants and Ms. Heather Miller for technical assistance in analyzing sequences.

REFERENCES

1. Denissenko, M. F., Pao, A., Pfeifer, G. P., and Tang, M. (1998) *Oncogene 16*, 1241−1247.
2. Hoare, S., Zou, Y., Purohit, V., Krishnasamy, R., Skorvaga, M., Van Houten, B., Geacintov, N. E., and Basu, A. K. (2000) *Biochemistry 39*, 12252−12261.
3. Kowalczyk, A., Carmical, J. R., Zou, Y., Van Houten, B., Lloyd, R. S., Harris, C. M., and Harris, T. M. (2002) *Biochemistry 41*, 3109−3118.
4. Mekhovich, O., Tang, M., and Romano, L. J. (1998) *Biochemistry 37*, 571−579.
5. Zou, Y., Crowley, D. J., and Van Houten, B. (1998) *J. Biol. Chem. 273*, 12887−12892.

6. Huang, Y. P., and Ito, J. (1998) *Nucleic Acids Res. 26*, 5300−5309.
7. Nelson, K. E., Clayton, R. A., Gill, S. R., Gwinn, M. L., Dodson, R. J., Haft, D. H., Hickey, E. K., Peterson, J. D., Nelson, W. C., Ketchum, K. A., McDonald, L., Utterback, T. R., Malek, J. A., Linher, K. D., Garrett, M. M., Stewart, A. M., Cotton, M. D., Pratt, M. S., Phillips, C. A., Richardson, D., Heidelberg, J., Sutton, G. G., Fleischmann, R. D., Eisen, J. A., White, O., Salzberg, S. L., Smith, H. O., Venter, J. C., and Fraser, C. M. (1999) *Nature 399*, 323−329.
8. Guengerich, F. P. (1992) *Pharmacol. Ther. 54*, 17−61.
9. Quan, T., Reiners, J. J., Jr., Culp, S. J., Richter, P., and States, J. C. (1995) *Mol. Carcinog. 12*, 91−102.
10. Jiang, G., Skorvaga, M., Van Houten, B., and States, J. C. (2003) *Protein Expr. Purif. 31*, 88−98.
11. Straub, K. M., Meehan, T., Burlingame, A. L., and Calvin, M. (1977) *Proc. Natl. Acad. Sci. U.S.A. 74*, 5285−5289.
12. Jiang, G., Jankowiak, R., Grubor, N., Banasiewicz, M., Small, G. J., Skorvaga, M., Van Houten, B., and States, J. C. (2004) *Chem. Res. Toxicol. 17*, 330−339.
13. Zou, Y., Luo, C., and Geacintov, N. E. (2001) *Biochemistry 40*, 2923−2931.
14. Zou, Y., Liu, T. M., Geacintov, N. E., and Van Houten, B. (1995) *Biochemistry 34*, 13582−13593.
15. DellaVecchia, M. J., Croteau, D. L., Skorvaga, M., Dezhurov, S. V., Lavrik, O. I., and Van Houten, B. (2004) *J Biol. Chem.*
16. Moolenaar, G. F., Visse, R., Ortiz-Buysse, M., Goosen, N., and van de, P. P. (1994) *J. Mol. Biol. 240*, 294−307.
17. Moolenaar, G. F., Bazuine, M., van Knippenberg, I. C., Visse, R., and Goosen, N. (1998) *J. Biol. Chem. 273*, 34896−34903.
18. Moolenaar, G. F., Monaco, V., van der Marel, G. A., van Boom, J. H., Visse, R., and Goosen, N. (2000) *J. Biol. Chem. 275*, 8038−8043.
19. Verhoeven, E. E., Wyman, C., Moolenaar, G. F., and Goosen, N. (2002) *EMBO J. 21*, 4196−4205.
20. Zou, Y., and Van Houten, B. (1999) *EMBO J. 18*, 4889−4901.
21. Moolenaar, G. F., Rossum-Fikkert, S., van Kesteren, M., and Goosen, N. (2002) *Proc. Natl. Acad. Sci. U.S.A. 99*, 1467−1472.
22. Van Houten, B., Eisen, J. A., and Hanawalt, P. C. (2002) *Proc. Natl. Acad. Sci. U.S.A. 99*, 2581−2583.
23. Tang, M., Nazimiec, M., Ye, X., Iyer, G. H., Eveleigh, J., Zheng, Y., Zhou, W., and Tang, Y. Y. (2001) *J. Biol. Chem. 276*, 3904−3910.
24. Nazimiec, M., Lee, C. S., Tang, Y. L., Ye, X., Case, R., and Tang, M. (2001) *Biochemistry 40*, 11073−11081.
25. Hess, M. T., Gunz, D., Luneva, N., Geacintov, N. E., and Naegeli, H. (1997) *Mol. Cell Biol. 17*, 7069−7076.
26. Jankowiak, R., Lin, C. H., Zamzow, D., Roberts, K. P., Li, K. M., and Small, G. J. (1999) *Chem. Res. Toxicol. 12*, 768−777.
27. Lu, P. Q., Jeong, H., Jankowiak, R., Small, G. J., Kim, S. K., Cosman, M., and Gracintov, N. E. (1991) *Chem. Res. Toxicol. 4*, 58−69.
28. Huang, W., Amin, S., and Geacintov, N. E. (2002) *Chem. Res. Toxicol. 15*, 118−126.
29. Xie, X. M., Geacintov, N. E., and Broyde, S. (1999) *Chem. Res. Toxicol. 12*, 597−609.
30. Delagoutte, E., Bertrand-Burggraf, E., Dunand, J., and Fuchs, R. P. (1997) *J. Mol. Biol. 266*, 703−710.
31. Delagoutte, E., Fuchs, R. P., and Bertrand-Burggraf, E. (2002) *J. Mol. Biol. 320*, 73−84.
32. Moolenaar, G. F., Herron, M. F., Monaco, V., van der Marel, G. A., van Boom, J. H., Visse, R., and Goosen, N. (2000) *J. Biol. Chem. 275*, 8044−8050.
33. Skorvaga, M., Theis, K., Mandavilli, B. S., Kisker, C., and Van Houten, B. (2002) *J. Biol. Chem. 277*, 1553−1559.
34. Verhoeven, E. E., van Kesteren, M., Turner, J. J., van der Marel, G. A., van Boom, J. H., Moolenaar, G. F., and Goosen, N. (2002) *Nucleic Acids Res. 30*, 2492−2500.
35. Moolenaar, G. F., Franken, K. L., van de, P. P., and Goosen, N. (1997) *Mutat. Res. 385*, 195−203.
36. Moolenaar, G. F., Franken, K. L., Dijkstra, D. M., Thomas-Oates, J. E., Visse, R., van de, P. P., and Goosen, N. (1995) *J. Biol. Chem. 270*, 30508−30515.
37. Verhoeven, E. E., van Kesteren, M., Moolenaar, G. F., Visse, R., and Goosen, N. (2000) *J. Biol. Chem. 275*, 5120−5123.

BI052515E